11-6-2015

Stress and Energy Transmission by Inhomogeneous Plane Waves into Dissipative Media

Daniel C. Woods
Purdue University, woods41@purdue.edu

J Stuart Bolton
Purdue University, bolton@purdue.edu

Jeffrey F. Rhoads
Purdue University, jfrhoads@purdue.edu

Stress and Energy Transmission by Inhomogeneous Plane Waves into Dissipative Media

Daniel C. Woods, J. Stuart Bolton,
and Jeffrey F. Rhoads

School of Mechanical Engineering,
Ray W. Herrick Laboratories,
and Birck Nanotechnology Center,
Purdue University
West Lafayette, Indiana, USA

November 6, 2015

Premise and Motivation

- Detection of improvised explosive devices (IEDs)
- Strong dependence of vapor pressure on temperature
  - May improve detection capabilities by selective heating

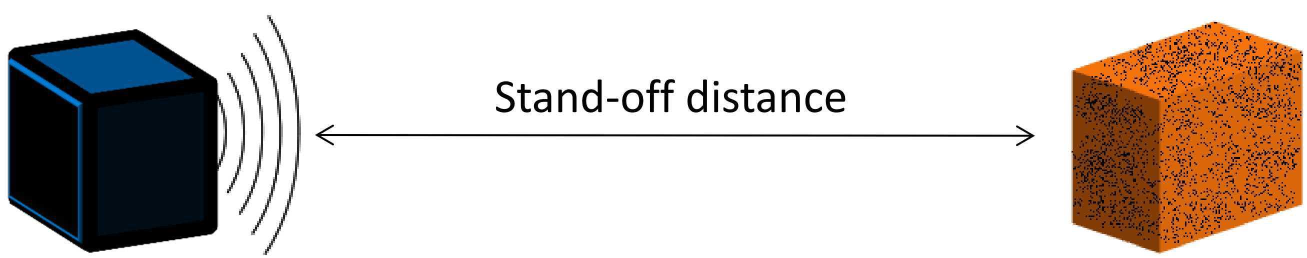

Low-frequency source

Energetic material
- Increase in temperature
- Increase in vapor pressure

Premise and Motivation

- Optimization of incident wave parameters for maximal stress and energy transmission
  - Theoretical study of incident inhomogeneous plane waves in dissipative media
  - Minimization of reflection coefficient magnitude

Basic representation of acoustical interface

General Acoustic Plane Waves

Homogeneous wave

Inhomogeneous wave

Ideal fluid or Elastic solid

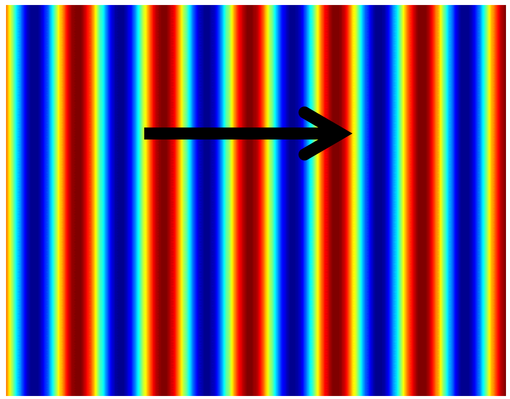

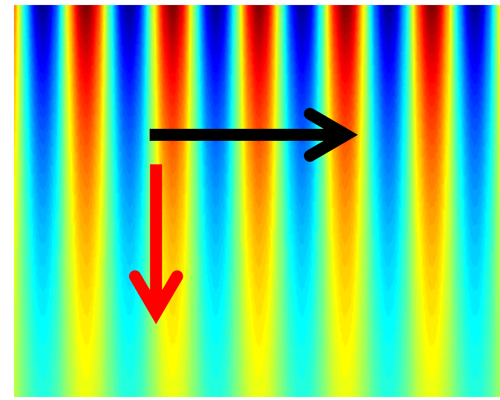

Real fluid or Viscoelastic solid

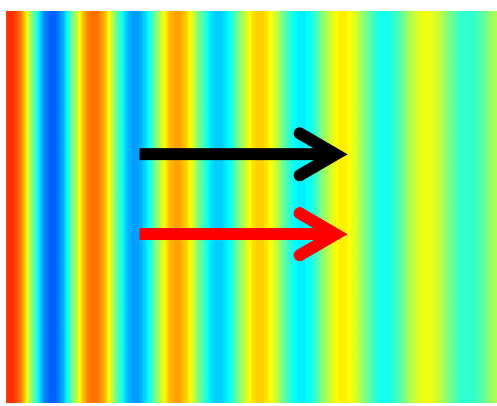

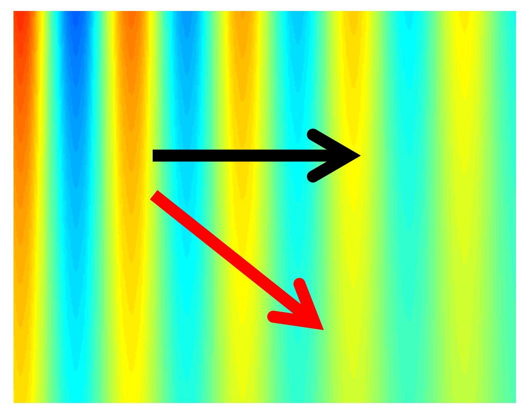

Representation in Dissipative Media

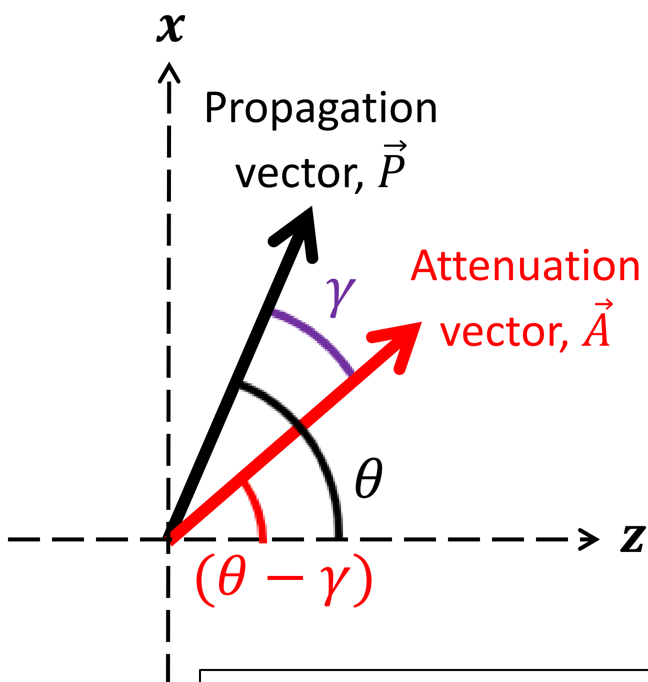

Wave inhomogeneity angle,
$0° \leq \gamma < 90°$

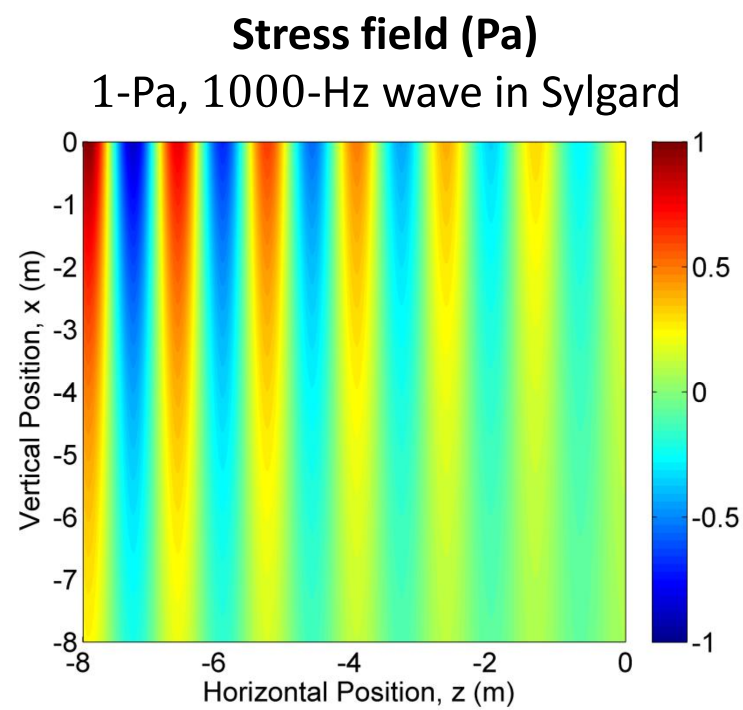

Representation in Dissipative Media

- Each wave type is characterized by the corresponding material wavenumber:

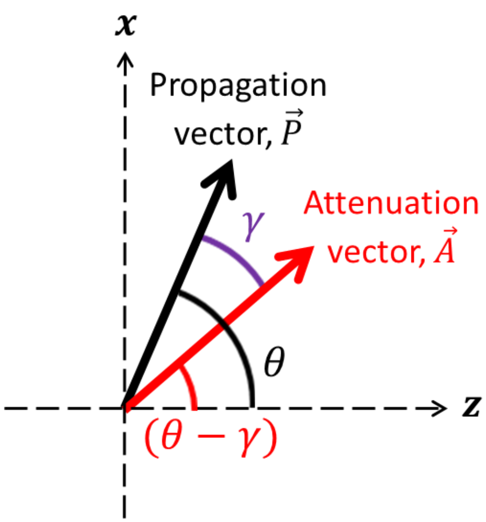

$$\tilde{k} = k_R + jk_I$$

  - Homogeneous waves ($\gamma = 0°$):

$$v_H = \frac{\omega}{k_R}, \qquad |\vec{A}_H| = -k_I$$

  - Inhomogeneous waves ($\gamma \neq 0°$):

$$v = \text{function}(\gamma) < v_H,$$
$$|\vec{A}| = \text{function}(\gamma) > |\vec{A}_H|$$

$$\tilde{k}_x = |\vec{P}|\sin(\theta) - j|\vec{A}|\sin(\theta - \gamma)$$
$$\tilde{k}_z = |\vec{P}|\cos(\theta) - j|\vec{A}|\cos(\theta - \gamma)$$

Creation of Inhomogeneous Plane Waves

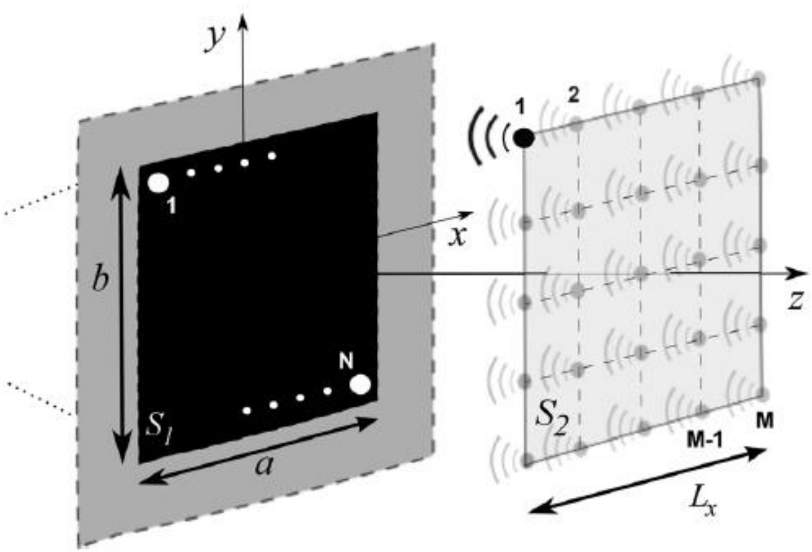

Phased arrays of sources
(*Robin et al., 2014*)

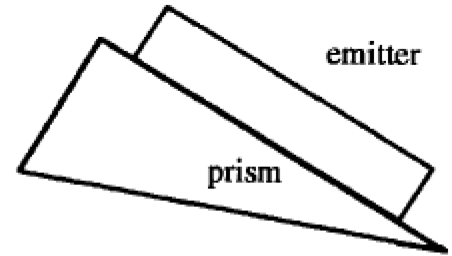

Selective absorbing geometries
(*Deschamps, 1994*)

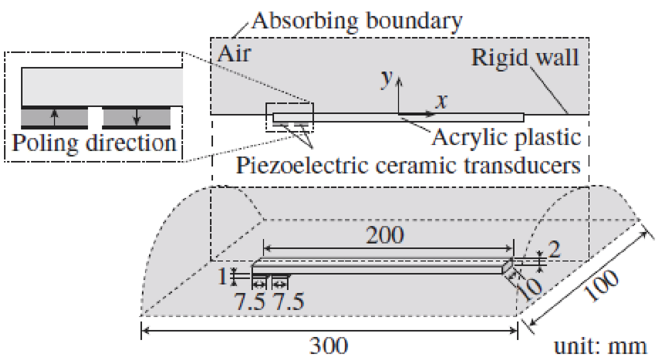

Vibrating plates coupled to piezoelectric transducers
(*Fujii et al., 2014*)

Fluid–Solid Interface

- Boundary conditions at interface ($z = 0$)

$$\sigma_{1,z}(x,0) = \sigma_{2,z}(x,0)$$

$$v_{1,z}(x,0) = v_{2,z}(x,0)$$

$$\sigma_{2,xz}(x,0) = 0$$

- Trace wavenumber continuity

$$\tilde{k}_{1,x} = \tilde{k}_{2,x} = \tilde{\kappa}_{2,x}$$

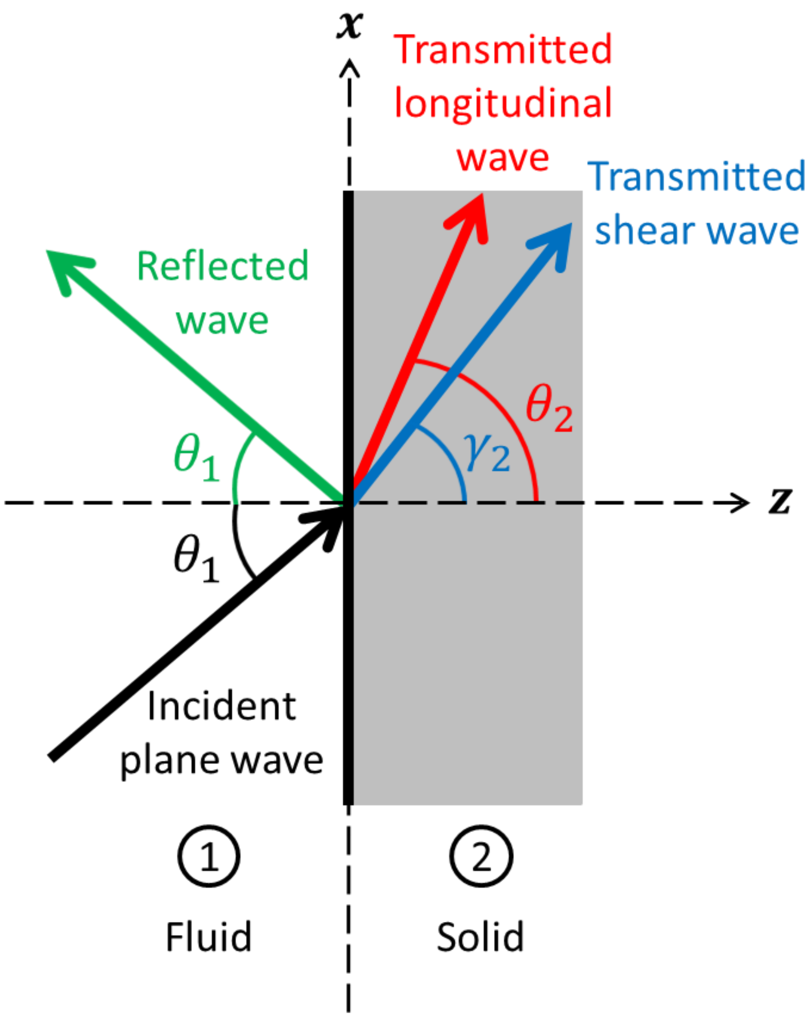

Optimal Incident Wave Parameters

- Optimal incidence angle is the Rayleigh angle

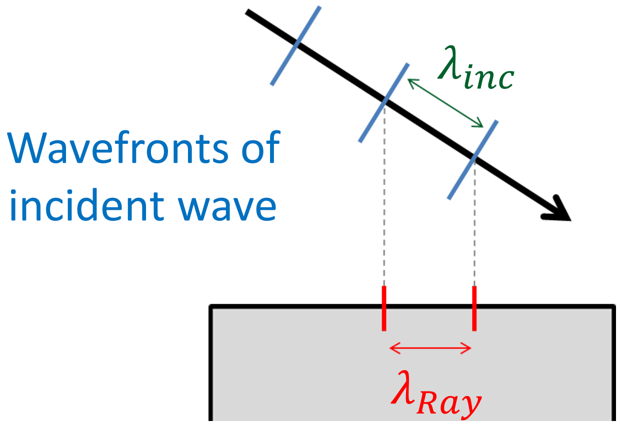

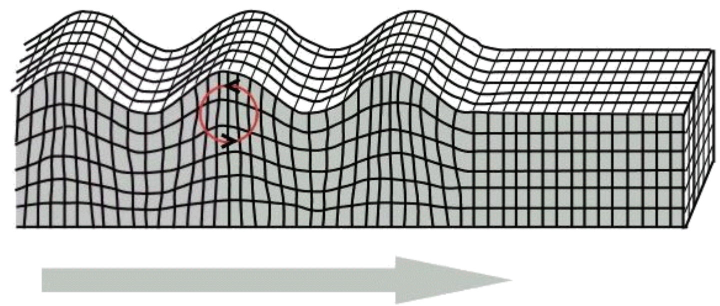

Spatial resonance of induced longitudinal and shear particle motions
(*image: http://www.sjvgeology.org/oil/Rayleigh_surface_waves2.gif)*

- Wave inhomogeneity:
  - For **low-loss solids**, optimal incident wave is ***inhomogeneous*** (unique such inhomogeneity)
  - For **higher-loss solids**, optimal incident wave is ***homogeneous***

Results for Ideal Fluid–Solid Interface

Magnitude of Reflection Coefficient
(1000 Hz)

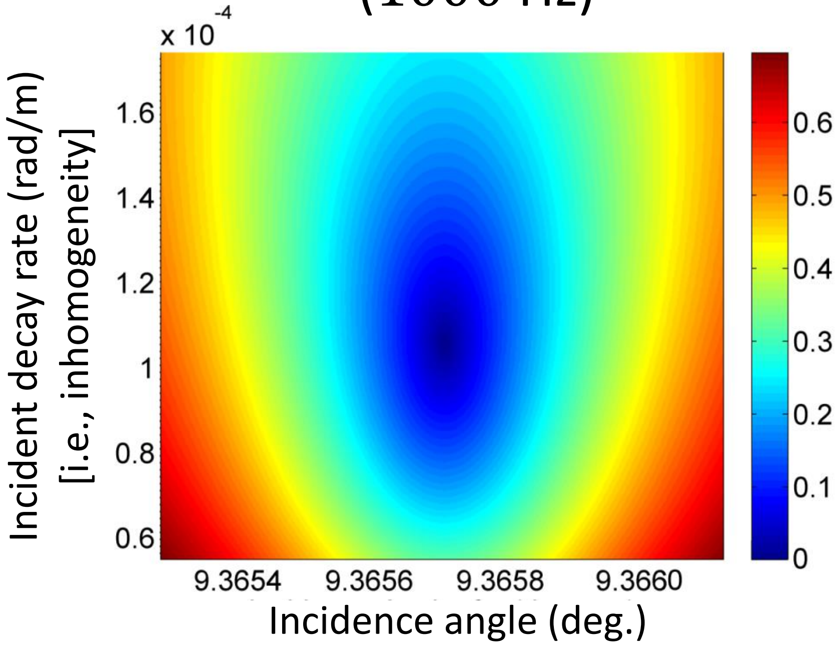

Stress Distribution in Elastic Solid (Pa)

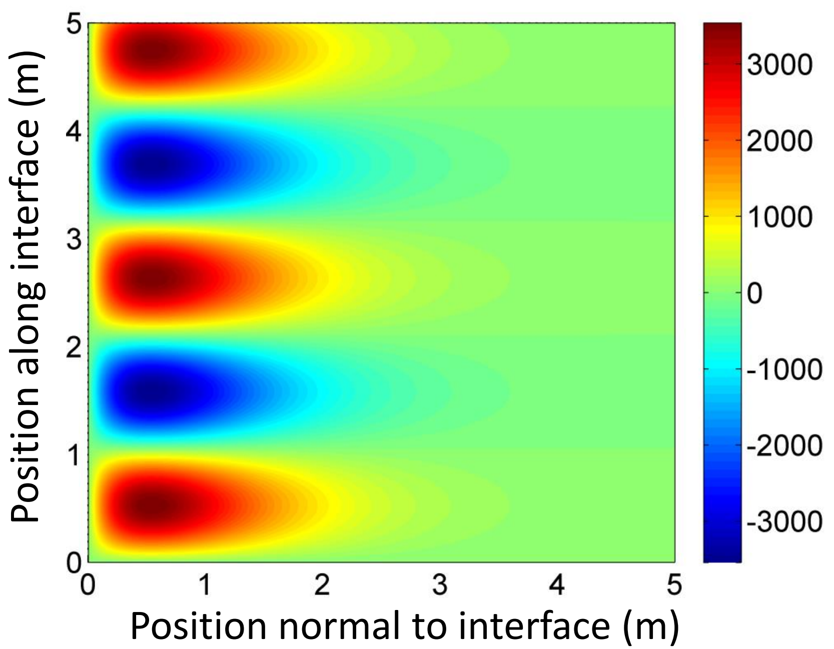

Low-Loss Interface: Water–Stainless Steel

Magnitude of Reflection Coefficient

Effect of Incidence Angle

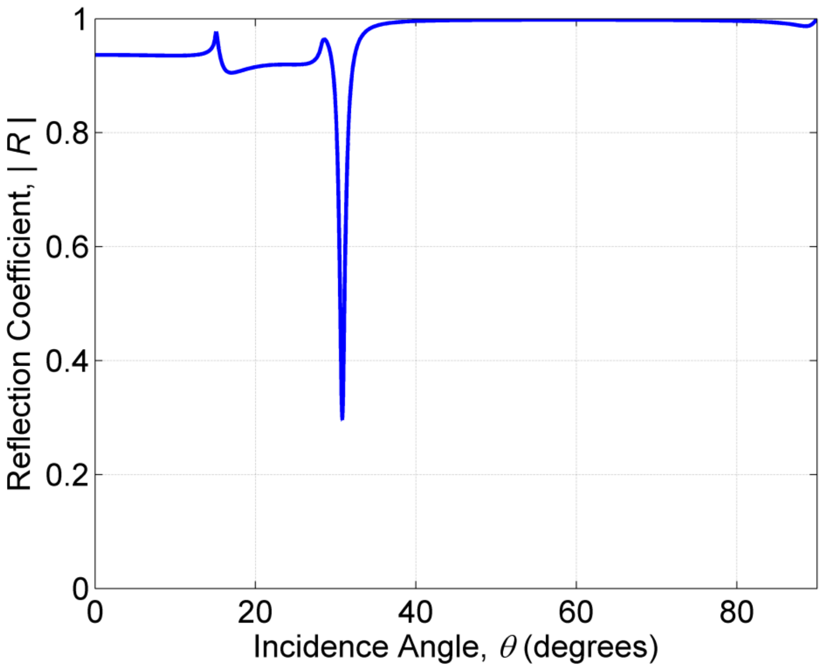

Effect of Wave Inhomogeneity (Near Rayleigh Angle)

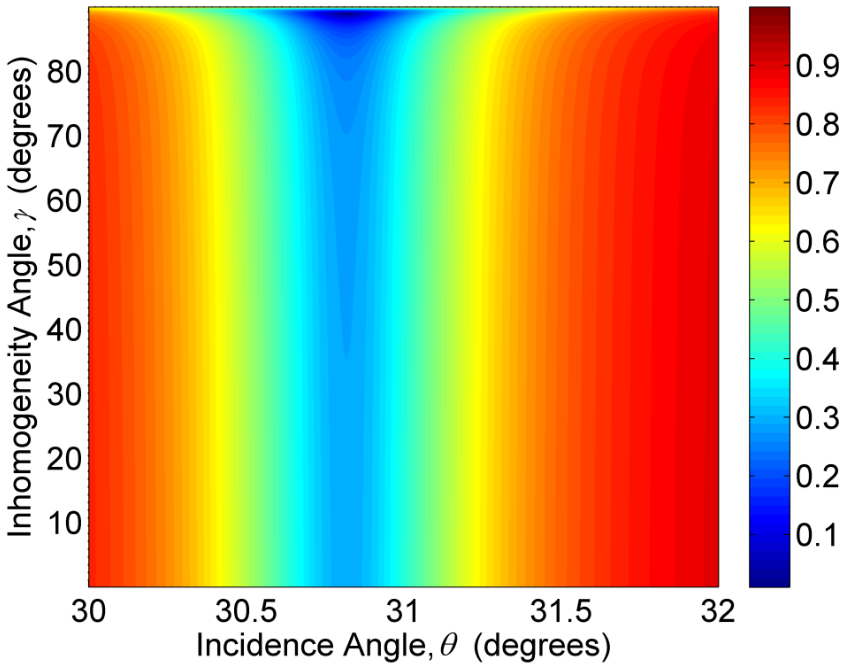

Low-Loss Interface: Water–Stainless Steel

Magnitude of Reflection Coefficient

Effect of Incidence Angle

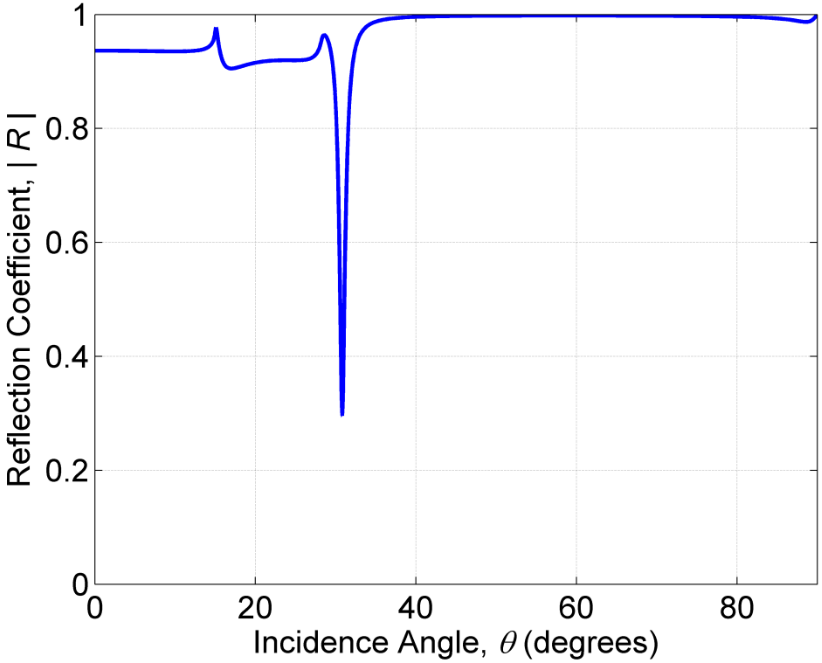

Effect of Wave Inhomogeneity (Near Rayleigh Angle)

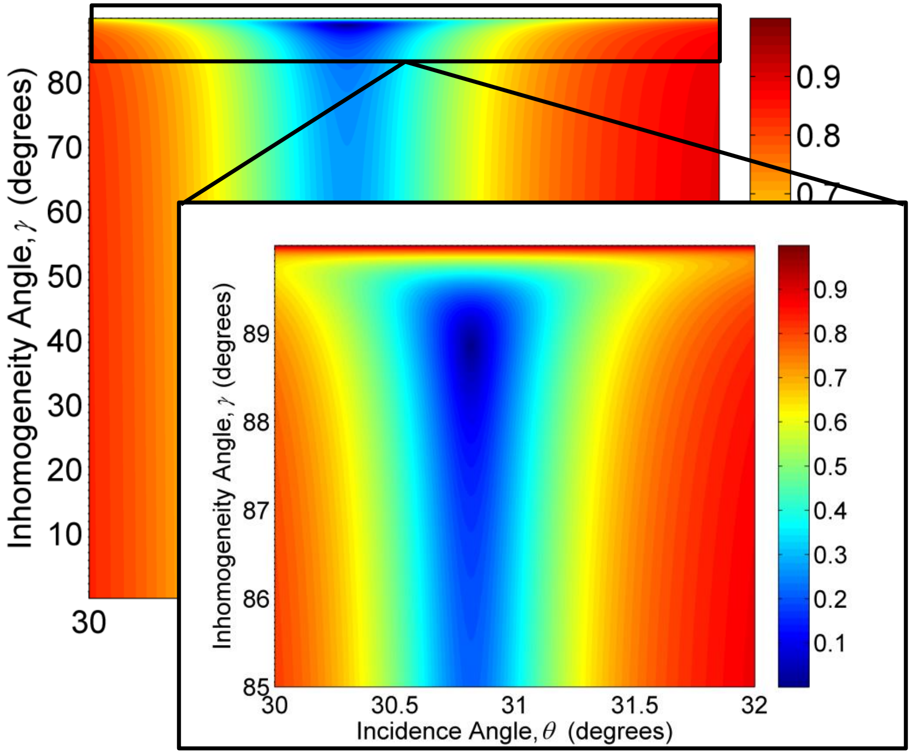

Effect of Increasing Material Dissipation

Magnitude of Reflection Coefficient
vs. Dissipation Level ($\theta \approx 30.82°$)

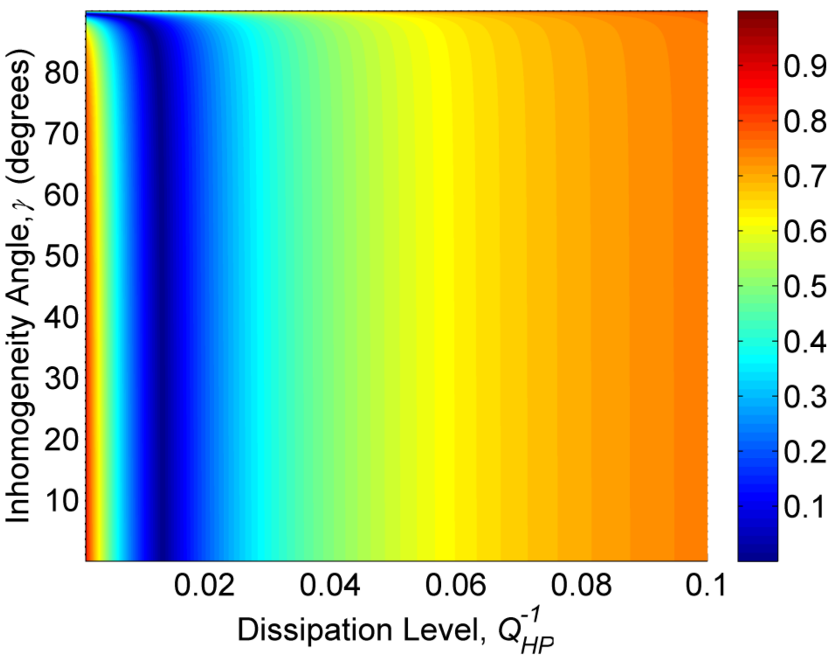

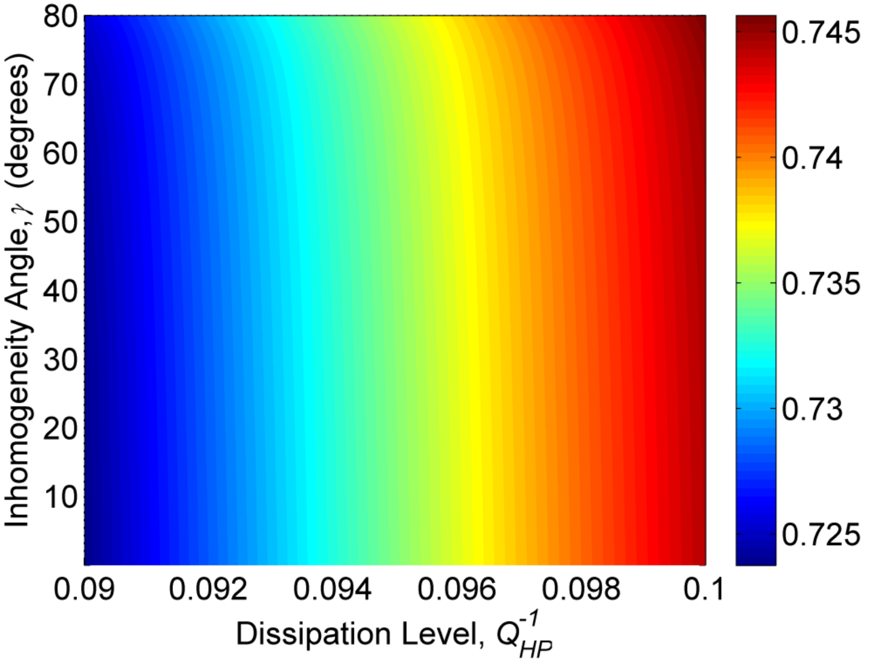

Low-Loss Interface: Water–Stainless Steel

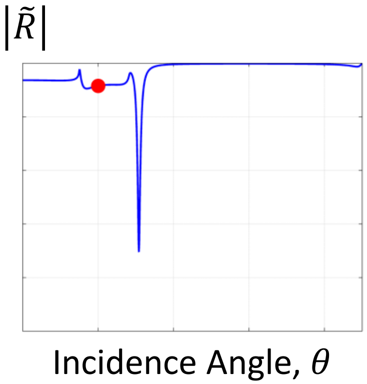

Transmitted Normal Stress Distribution

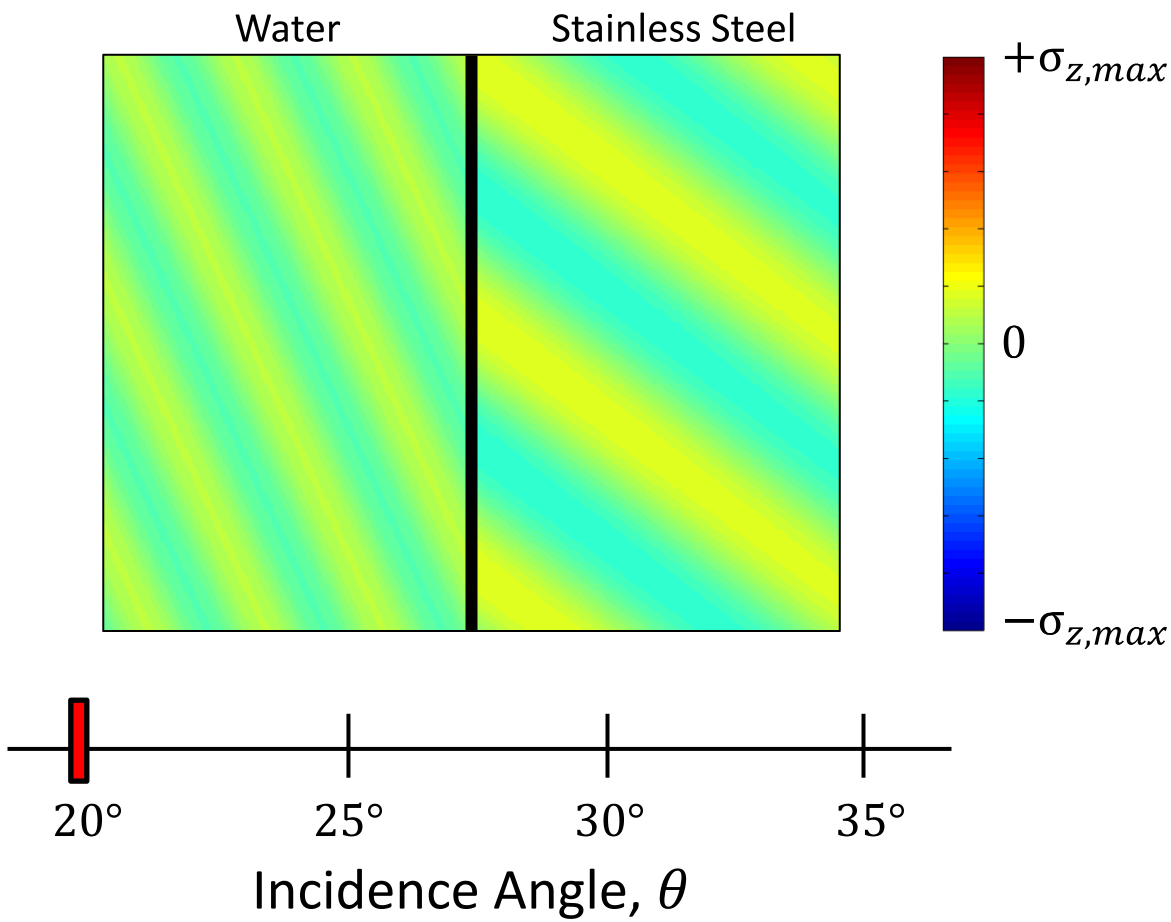

Low-Loss Interface: Water–Stainless Steel

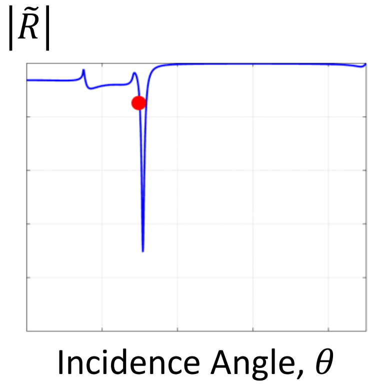

Transmitted Normal Stress Distribution

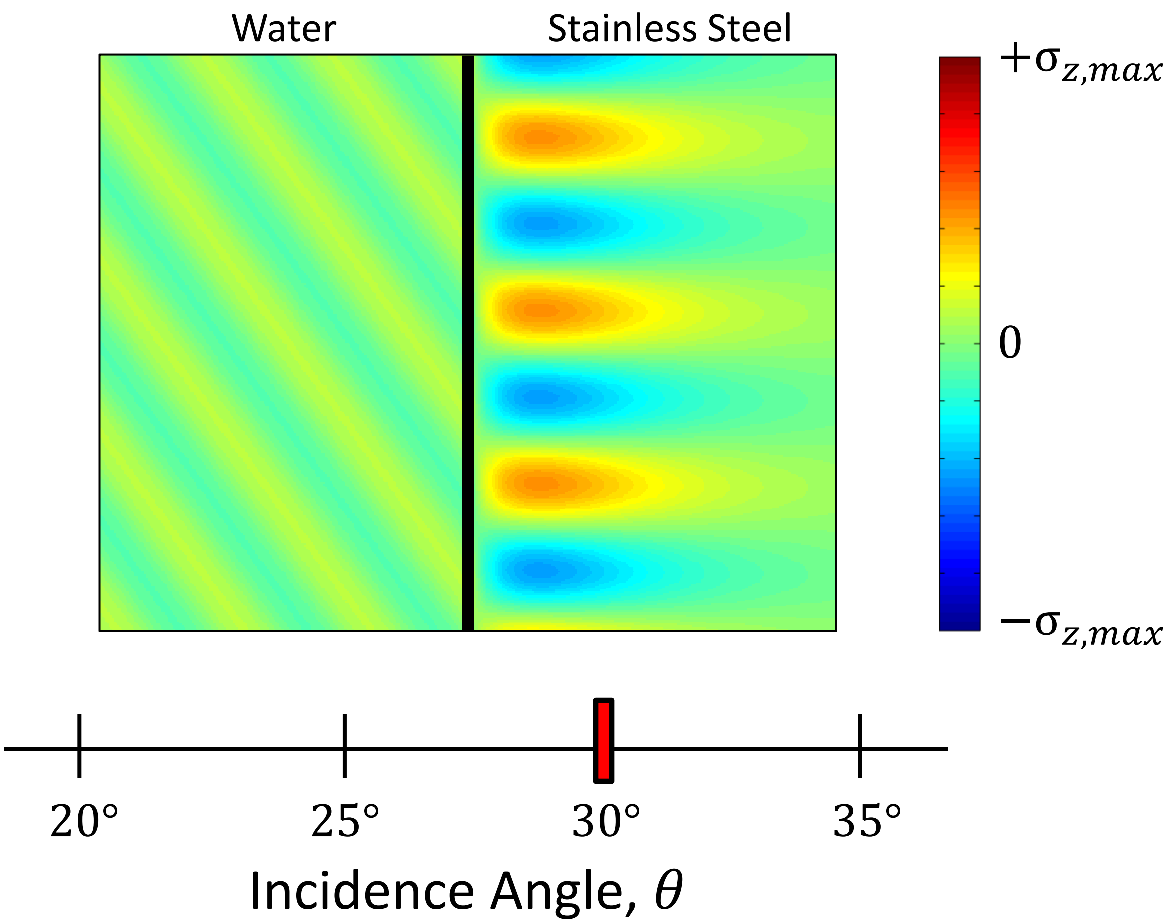

Low-Loss Interface: Water–Stainless Steel

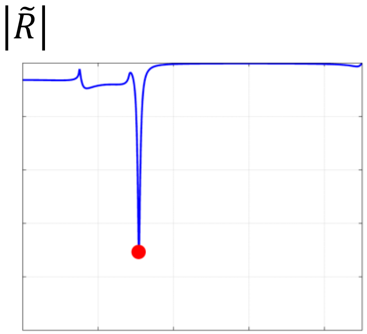

Incidence Angle, θ

Transmitted Normal Stress Distribution

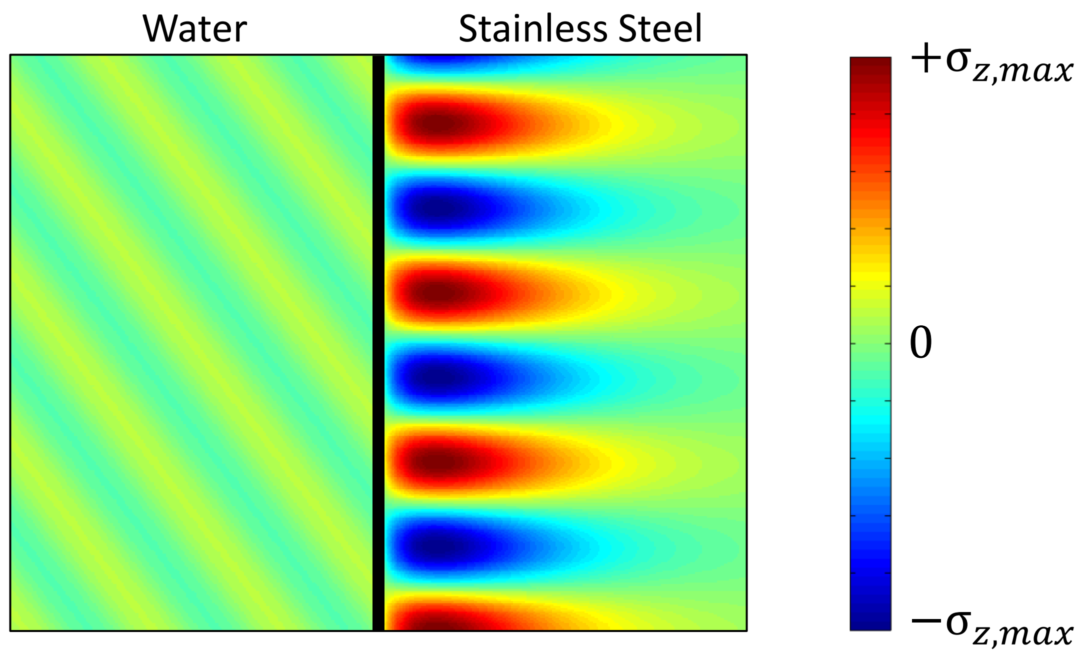

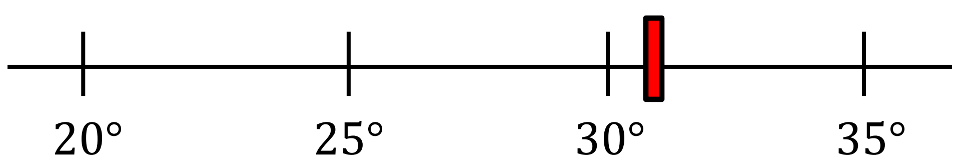

Incidence Angle, θ

Low-Loss Interface: Water–Stainless Steel

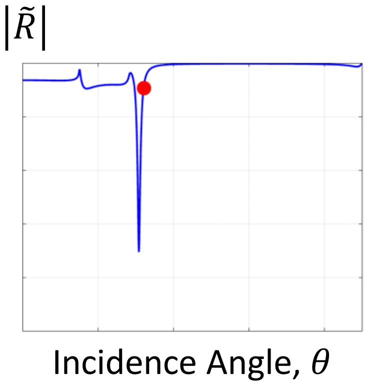

Transmitted Normal Stress Distribution

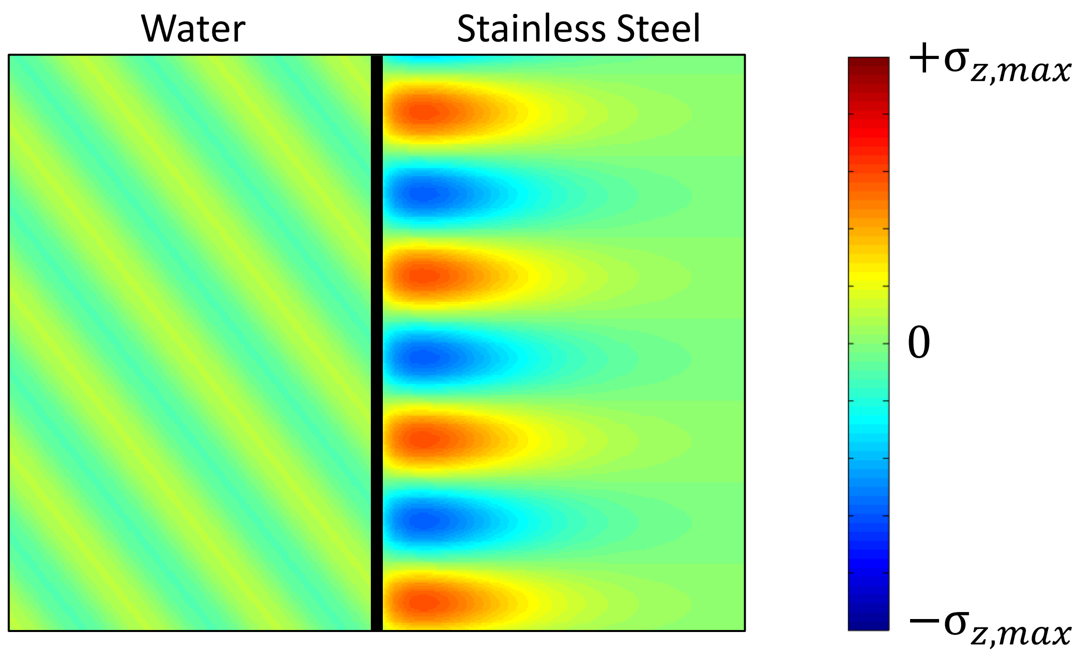

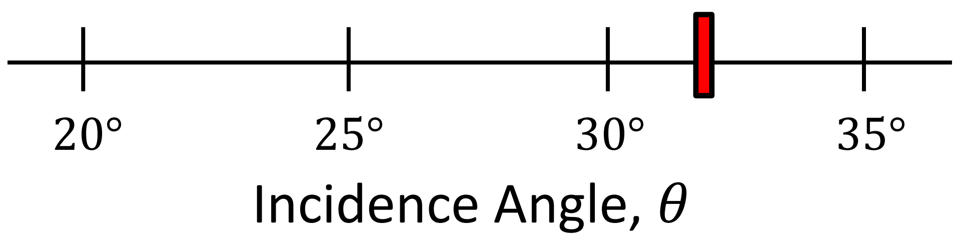

Low-Loss Interface: Water–Stainless Steel

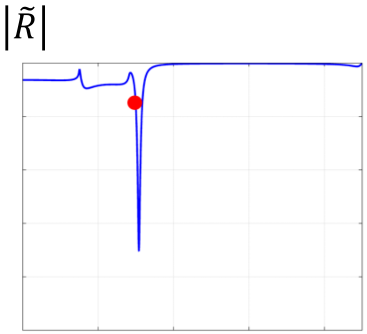

Incidence Angle, θ

Transmitted Normal Intensity Distribution

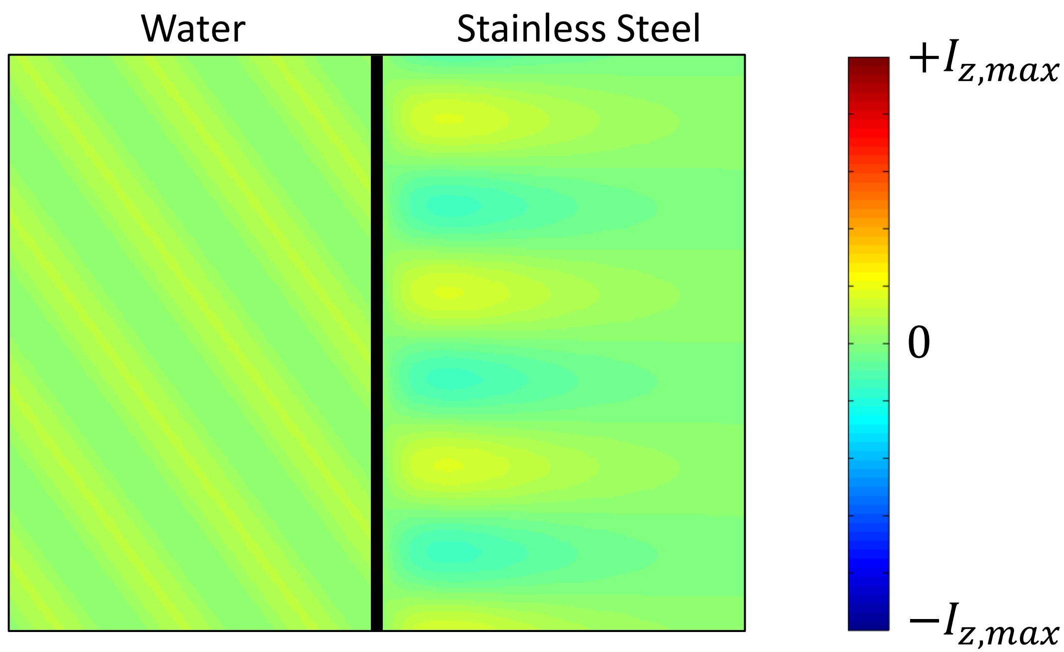

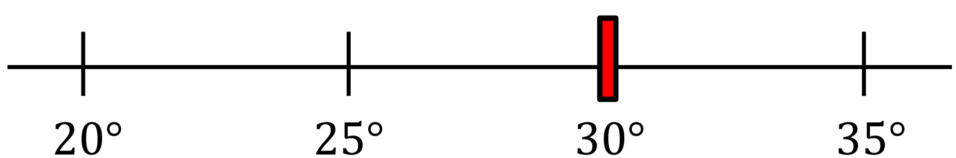

Incidence Angle, θ

Low-Loss Interface: Water–Stainless Steel

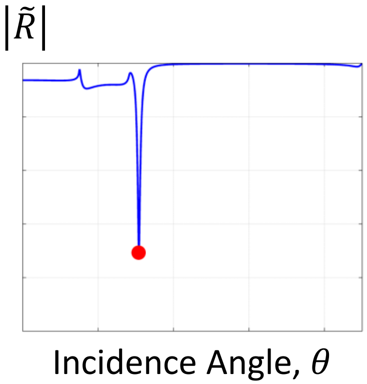

Transmitted Normal Intensity Distribution

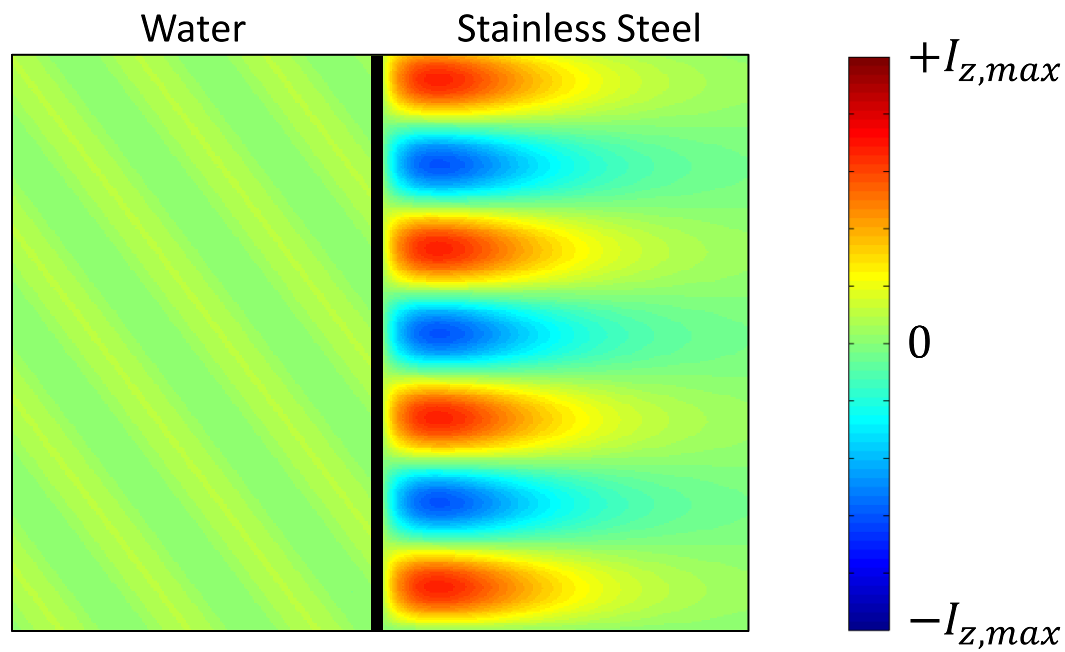

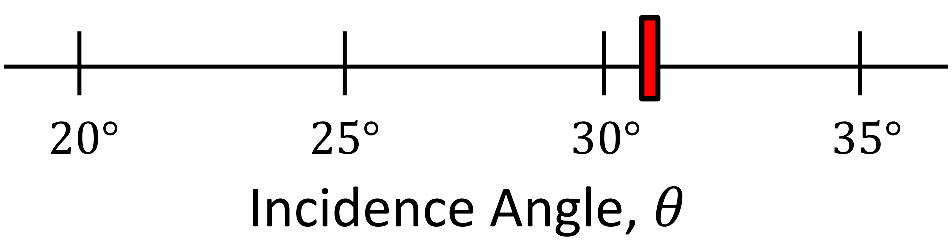

Low-Loss Interface: Water–Stainless Steel

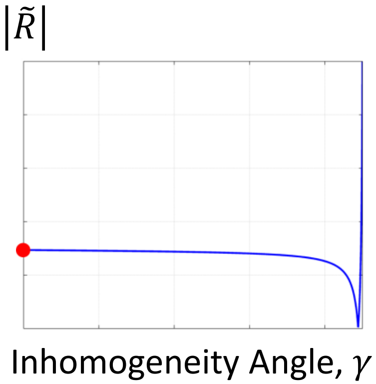

Transmitted Normal Intensity Distribution

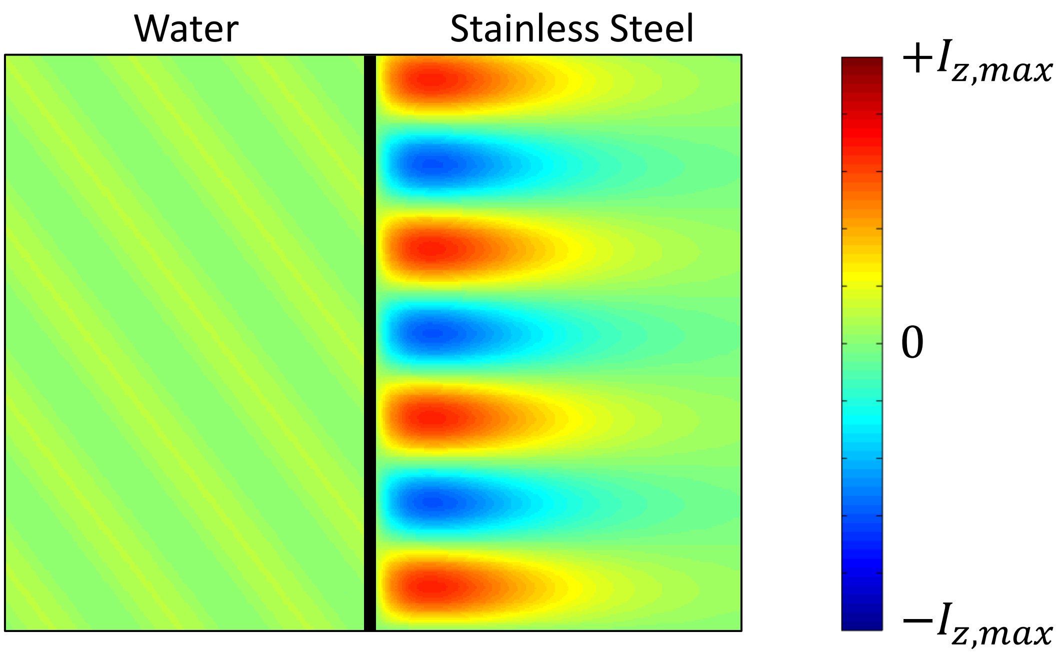

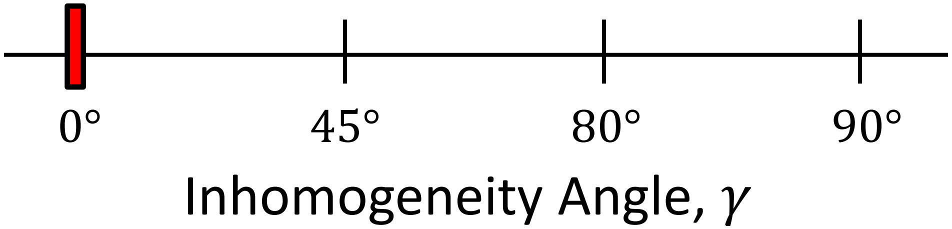

Low-Loss Interface: Water–Stainless Steel

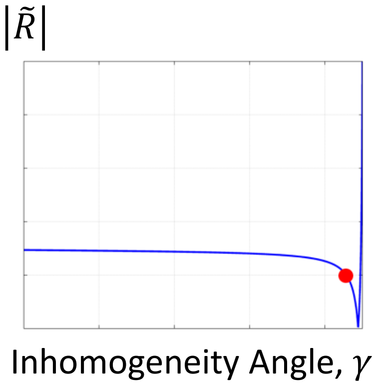

Transmitted Normal Intensity Distribution

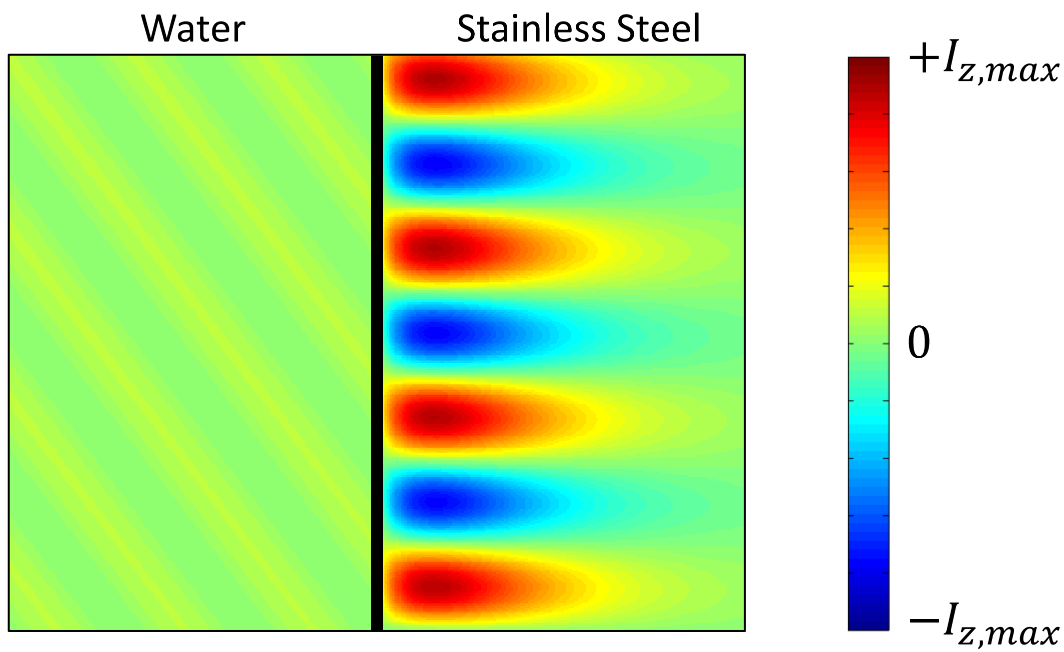

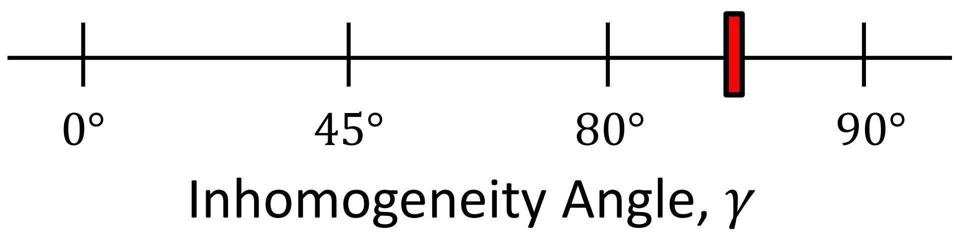

Low-Loss Interface: Water–Stainless Steel

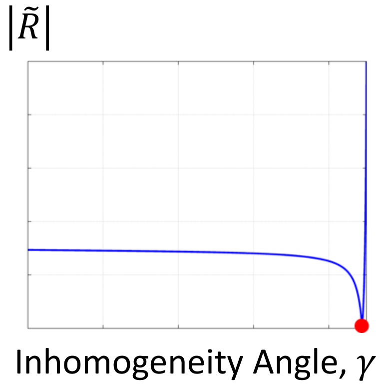

Transmitted Normal Intensity Distribution

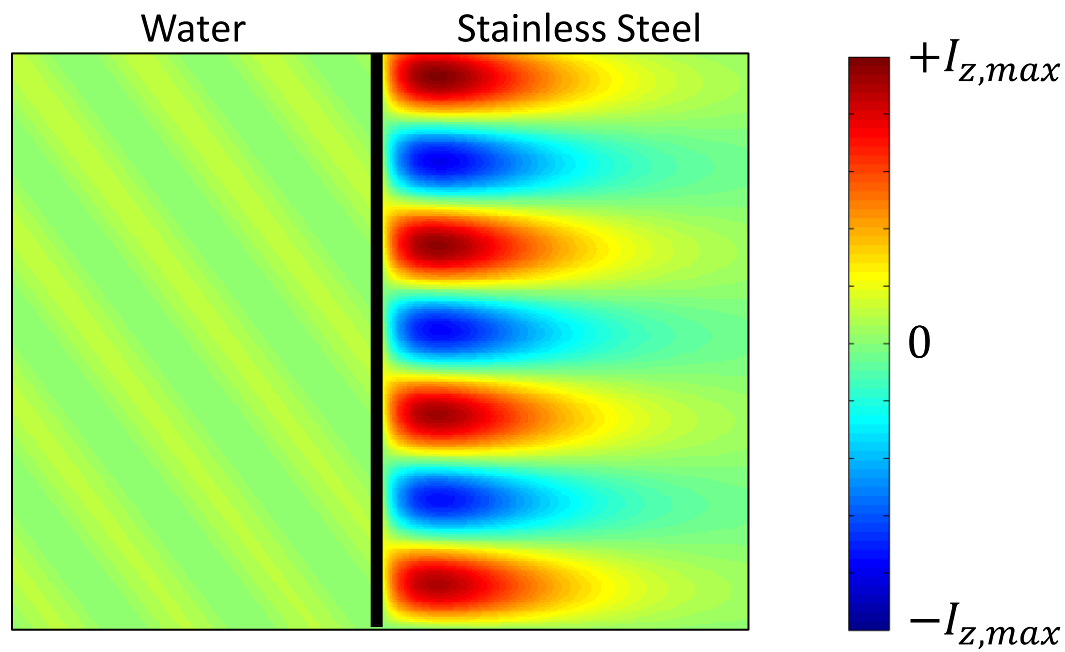

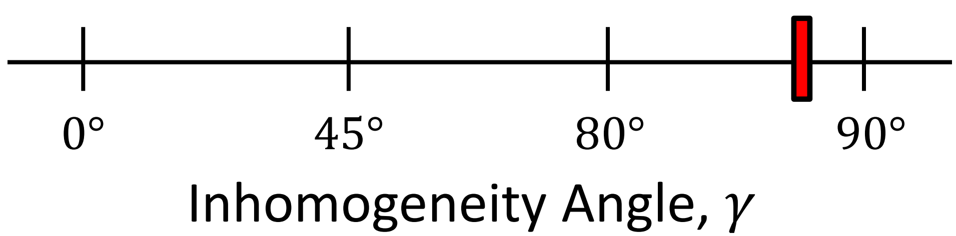

High-Loss Interface: Air–Sylgard

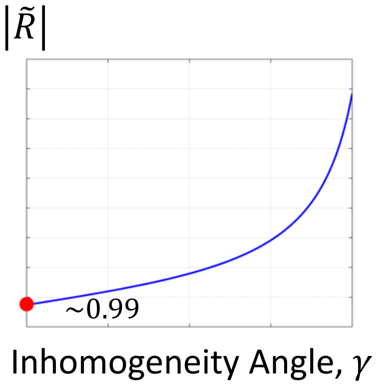

Transmitted Normal Stress Distribution

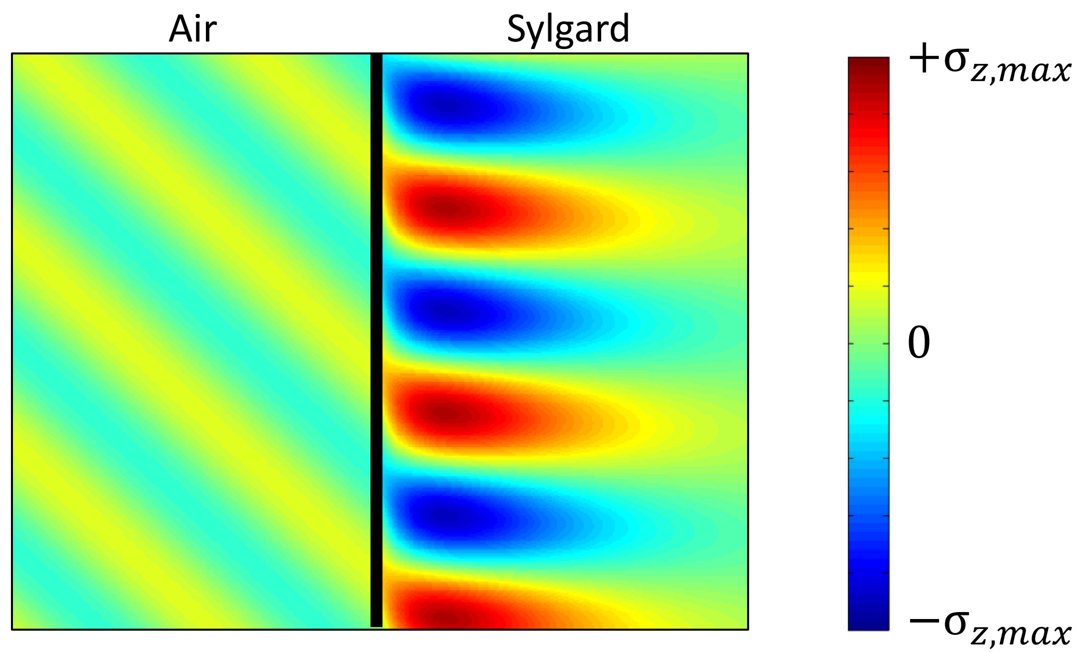

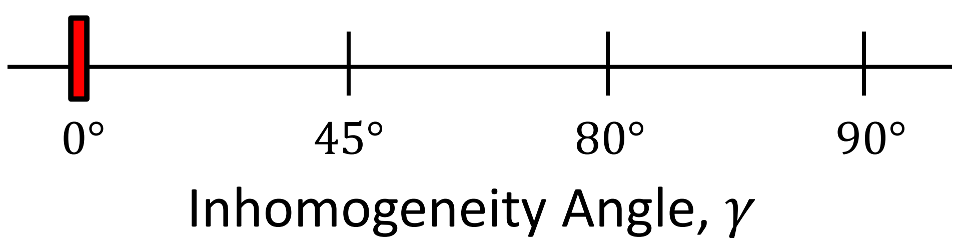

High-Loss Interface: Air–Sylgard

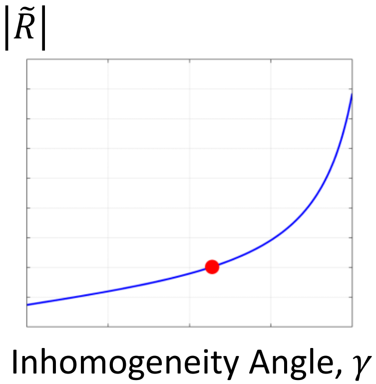

Transmitted Normal Stress Distribution

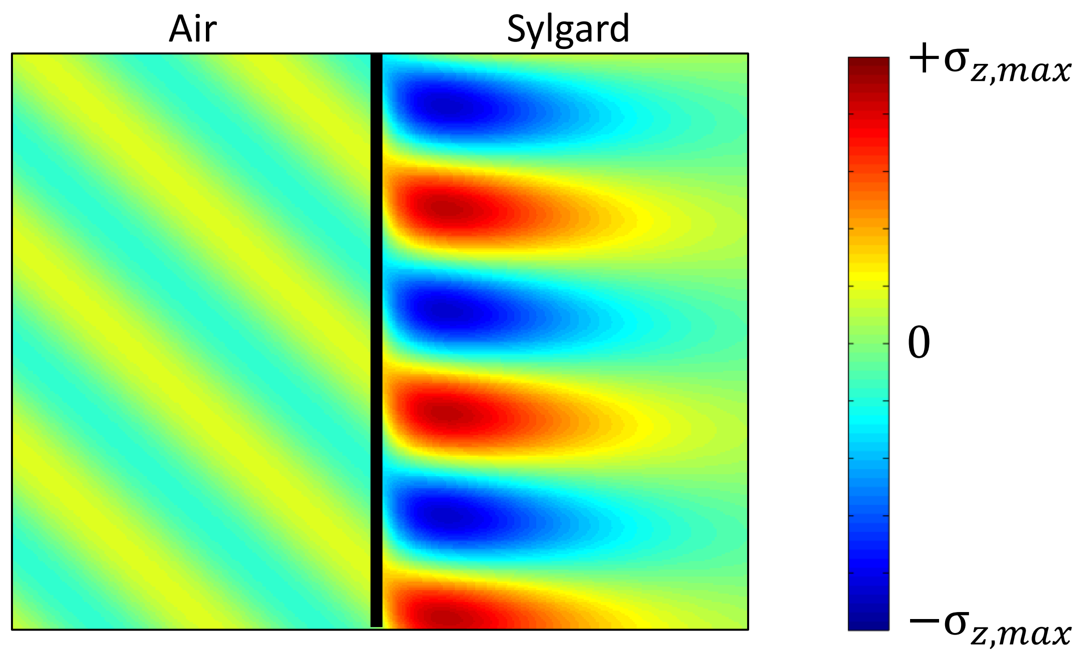

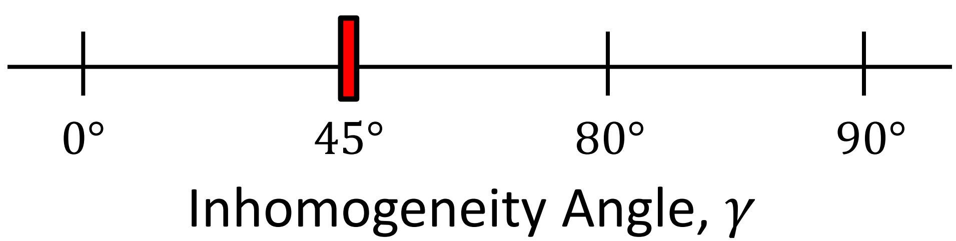

High-Loss Interface: Air–Sylgard

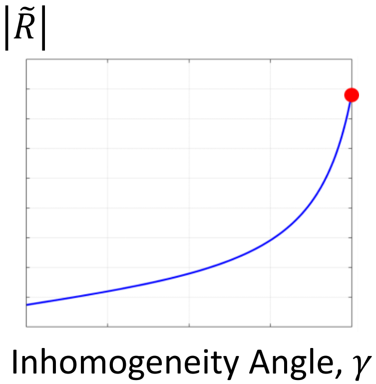

Transmitted Normal Stress Distribution

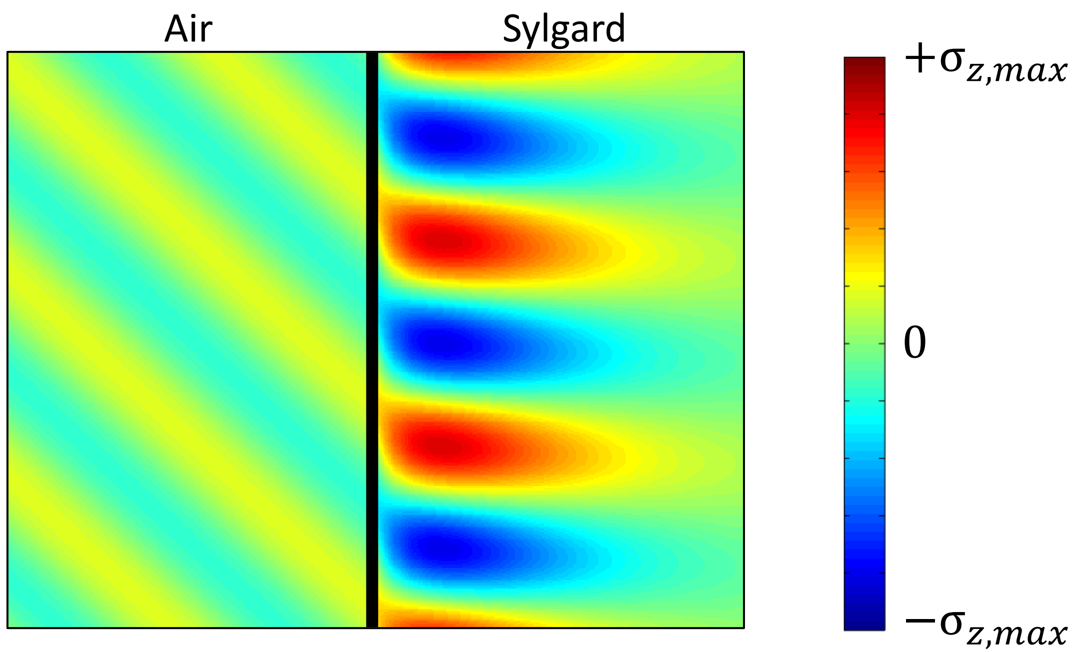

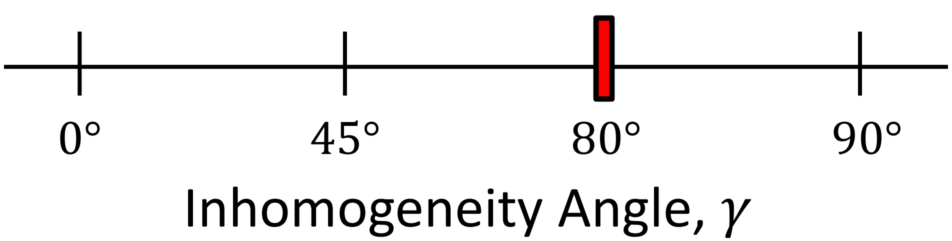

Conclusions

- Use of general acoustic plane waves for increased transmission in solids

Interface	Optimal incident wave	Attainable energy transmission
Ideal fluid–Elastic solid	• Inhomogeneous • At Rayleigh angle	• Total transmission • Reflection $\rightarrow 0$ • Narrow domain
Real fluid–Viscoelastic solid	• Inhomogeneous for low-loss solids • Homogeneous for high-loss solids	• Less than total transmission • Reflection > 0 • Wider domain

Next Steps

- Further characterization of transmission into viscoelastic materials of interest
  - Polymer-bonded energetic materials
- Transmission by finite, spatially-distributed waves
  - Bounded wave profiles typically used in practice
  - Various spatial distributions

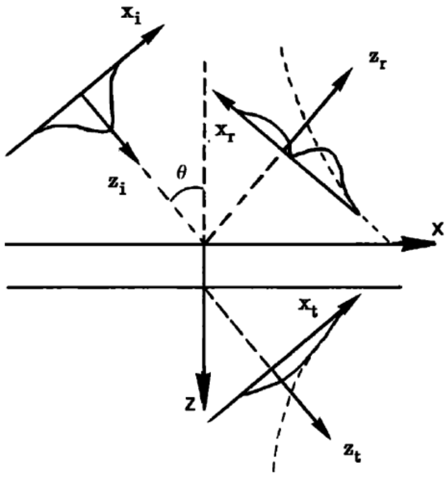

(*Van Den Abeele & Leroy, 1993*)

Acknowledgement

The authors would like to thank the U.S. Office of Naval Research for its support of this research under ONR Grant No. N00014-10-1-0958

Results for Ideal Fluid–Solid Interface

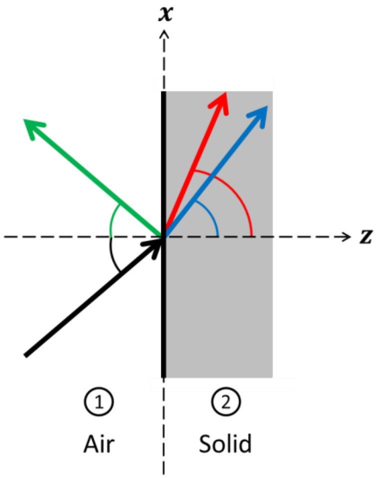

Transmitted Normal Intensity (W/m^2)

1-Pa, 1000-Hz incident wave

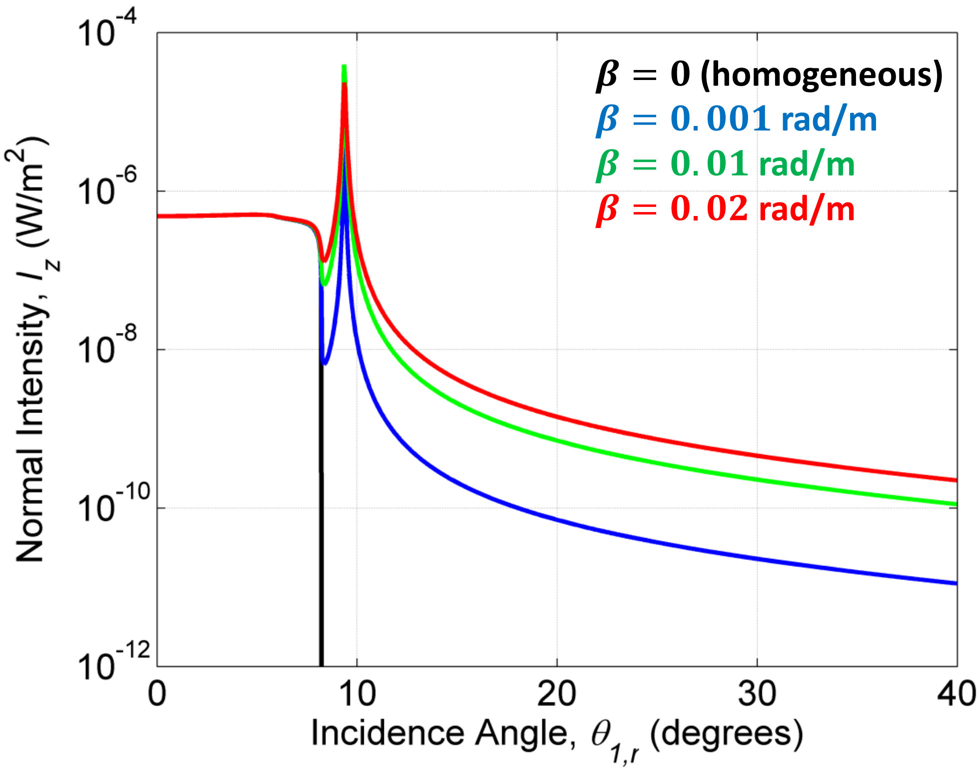

Sample solid

$\rho = 1000\rho_{air}$

$c = 10c_{air}$

$b = 7c_{air}$

$$I_z = \frac{1}{T}\int_0^T -(\sigma_z v_z + \sigma_{xz} v_x)\,dt$$

Results for Ideal Fluid–Solid Interface

Transmitted Normal Stress (Pa)

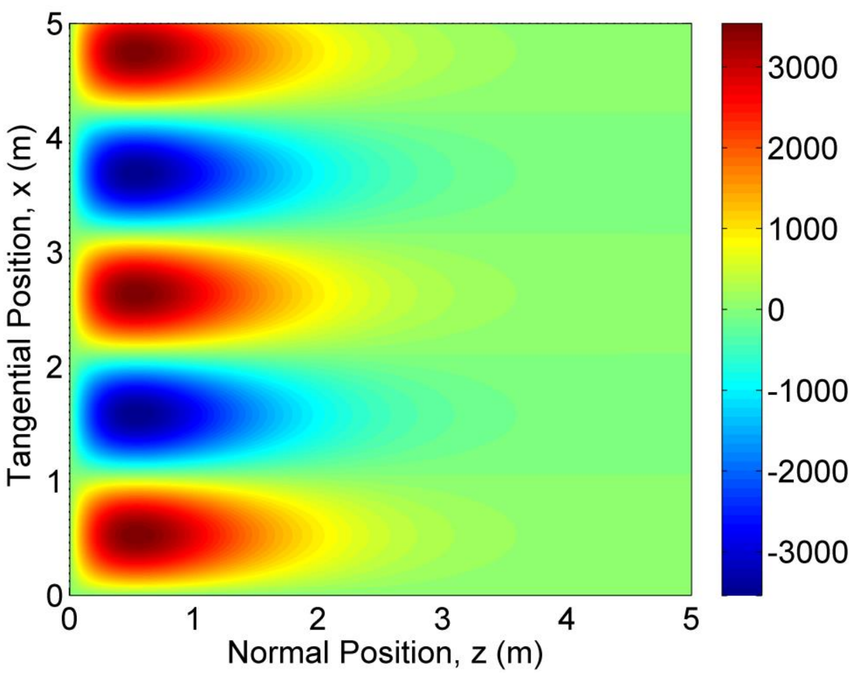

Transmitted Normal Velocity (m/s)

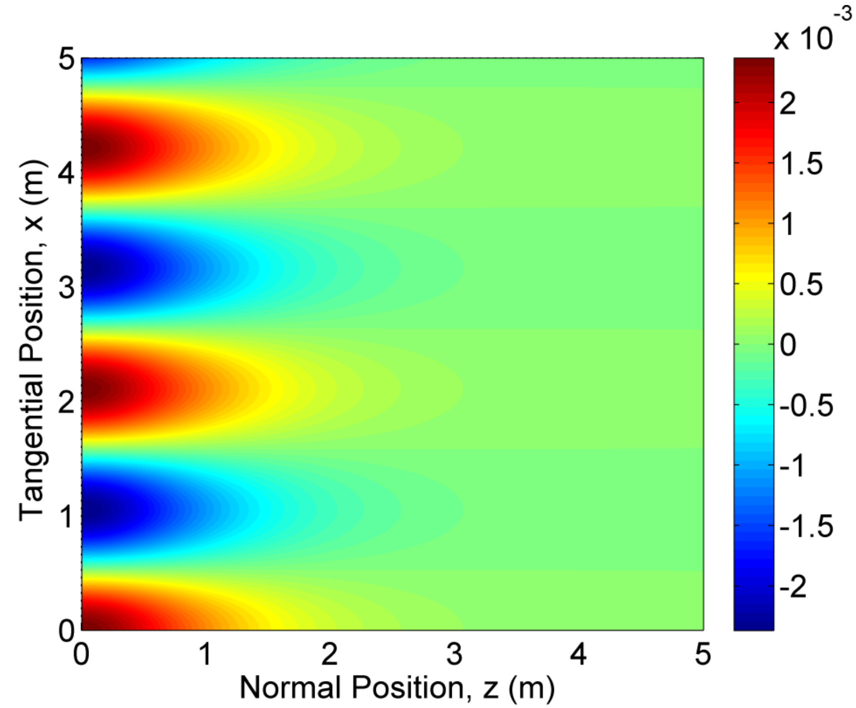

Approximate parameters for $|\widetilde{R}| = 0$

$\theta_{1,r}^{*} \approx 9.3657°, \beta^{*} \approx 1.07 \times 10^{-4}$ rad/m

Results for Ideal Fluid–Solid Interface

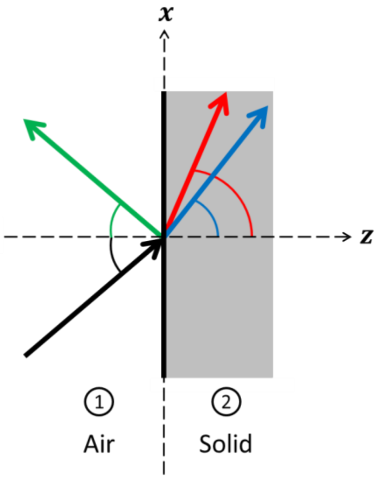

Transmitted Normal Intensity (W/m^2)

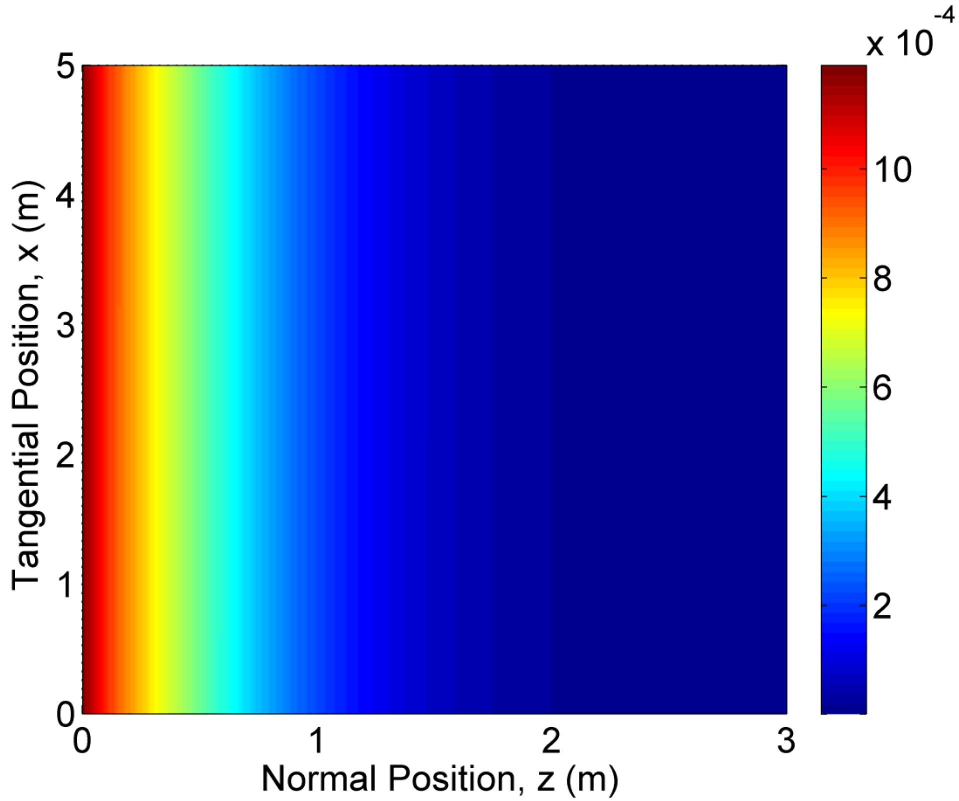

Compare with $\sim 5 \times 10^{-7}$ W/m² for homogeneous waves below the critical angle